Available online at www.derpharmachemica.com

ISSN 0975-413X
CODEN (USA): PCHHAX

Der Pharma Chemica, 2016, 8(4):243-250
(http://derpharmachemica.com/archive.html)

Luminescent and Gas Sensing Properties of SnO_2 Thin Films Grown by Pulsed Laser Deposition

M. C. Rao[1*], K. Ravindranadh[2], T. Satyanarayana[3], Y. Dasaradhudu[4], G. Nagarjuna[5], K. Srinivas[5] and M. S. Shekhawat[6]

[1]*Department of Physics, Andhra Loyola College, Vijayawada – 520008, India*
[2]*Physics Division, Department of Basic Sciences & Humanities, Chirala Engineering College, Chirala-523 157, India*
[3]*Department of EIE, Lakireddy Bali Reddy College of Engineering, Mylavaram- 521230, India*
[4]*Department of Physics, S. V. Arts College, Tirupati - 517502, India*
[5]*Department of Chemistry, S. R. R. & C. V. R. Govt. College, Vijayawada-520 004, India*
[6]*Department of Physics, Engineering College Bikaner, Bikaner - 334004, India*

ABSTRACT

SnO_2 films have a wide range of applications because of their excellent performance along with high mechanical, chemical and environmental stability and low cost material. SnO_2 thin films were prepared by pulsed lased deposition method. SEM, EDS, TEM, PL, Gas sensing and Electrical properties were carried out on to the prepared thin films. SEM images reveal that the sample consists of irregular shaped sphere like structures. EDS pattern showed the elemental compositions of Sn and O. TEM measurements were performed to confirm the nanocrystalline nature of the samples and to study the morphology of the particles. PL studies of SnO_2 thin films exhibit blue emission bands. The thermo emf of SnO_2 thin films increased with the increasing of temperature. At low temperatures the Seebeck coefficient is observed to be high and the Seebeck coefficient decreases with increasing of temperature.

Keywords: SnO_2, Pulsed Laser Deposition, TEM, Gas sensing and Thermo emf.

INTRODUCTION

In recent years, there has emerged significant interest in the epitaxial growth and properties of functional oxide thin films [1]. Functional oxide of interest includes superconductors [2], ferroelectrics [3], dielectrics [4], phosphors [5] and semiconductors [6]. The latter class of oxides, namely semiconductors, has emerged as particularly interesting for sensors, thin-film electronics, and photonics. Tin oxide (SnO_2) is a wide band gap (3.6 eV) metal oxide semiconductor with excellent optical transparency in the visible range [7]. It possesses the rutile (tetragonal) crystal structure with a = 4.738 A˚ and c = 3.188 A˚. With a relatively high conductivity, visible wavelength transparency, chemical stability and thermal stability in oxidizing environments, tin oxide films are being explored for a number of applications. As a wide band gap semiconductor, SnO_2 is attractive for use in photonic applications, such as solar cells, where transparent electrodes are required [8]. SnO_2 thin films are used for gas sensor devices based on changes in conductivity when exposed to selected chemical species [9].

SnO_2 films have a wide range of applications because of their excellent performance along with high mechanical, chemical and environmental stability and low cost material. In addition, there is also interest in the possibility of inducing ferromagnetism in SnO_2 through transition metal doping, an approach that is also being pursued for other wide band gap semiconductors [10]. SnO_2 thin films have been fabricated by a variety of techniques including sol–gel method [11], electron beam evaporation [12], reactive sputtering [13] chemical vapor deposition [14] and sputtering [15]. One of the major challenges in synthesizing SnO_2 thin films is to control oxygen stoichiometry. When deposition is carried out in vacuum at high temperatures, SnO_2 films tend to be nonstoichiometric, frequently resulting in the formation of metastable phases such as SnO or Sn_3O_4. The existence of these metastable phases and relaxed crystal defects will strongly affect the properties of the films. While previous applications of SnO_2 for sensors or transparent conductors have primarily relied on polycrystalline material, many of the emerging applications for functional wide band gap semiconductors require highly crystalline epitaxial films. As such, understanding the effects of growth parameters and substrate selection on the epitaxial growth of SnO_2 is important.
Pulsed laser deposition (PLD) is widely used in the synthesis of complex oxide thin films [16]. Pulsed laser deposition has the advantage of operating in a reactive atmosphere over a wide range of oxygen pressure. The effects of growth parameters on the crystalline orientation, electrical transport properties and surface morphology is discussed. PLD is a powerful and flexible technique for fabricating simple and complex metal oxide films and has several advantages for thin film deposition: (i) Direct stoichiometry transfer from the target to the growing film, (ii) High deposition rate and inherent simplicity for the growth of multilayered structures, (iii) Dense, textured films can be produced more easily by PLD with in situ substrate heating. When PLD is carried out in the atmosphere of a chemically reactive gas (a process known as Reactive Pulsed Laser Deposition (RPLD)), the flux of the laser ablated material interacts with the gas molecules all along the transit from the target to the collector surface. The resulting deposited layer was found to have a chemical composition substantially the same as the base or starting material. In thin film deposition, the substrate temperature plays the important role of determining the thermo emf of films. In this study, we have deposited SnO_2 thin films and investigated the microstructural and gas sensing properties of the deposited thin films.

MATERIALS AND METHODS

SnO_2 thin films were grown by pulsed laser deposition technique. The ablation target was fabricated using high purity SnO_2 (99.99 %). The mixture was crushed and pressed at 5 tonns/cm^2 to make tablets of 3 mm thick and 13 mm diameter. To get quite robust targets, the tablets were sintered in air at 1100 ^{0}C. The typical substrates i.e. Si wafers were cleaned using HF solution. The target was rotated at 10 rotations per minute with an electric motor to avoid depletion of material at any given spot. The laser used in these experiments is the 248 nm line of a KrF excimer laser (Luminics PM 882) with 10 ns pulse with a repetition rate of 10 Hz. The rectangular spot size of the laser pulse was 1x3 mm^2 and the energy 300 mJ. The target substrate distance was 4 cm [17-19]. The deposition temperature was maintained with thermocouple and temperature controller. During the deposition pure oxygen was introduced into the deposition chamber and desired pressure was maintained with a flow controller [20-22].

Scanning electron microscope (SEM) and energy dispersive spectrum (EDS) images are taken on ZEISS EVO 18. Transmission electron microscope (TEM) images are recorded on HITACHI H-7600 and CCD CAMERA system AMTV-600 by dispersing samples in ethanol. Photoluminescence (PL) spectrum is taken at room temperature on Horiba Jobin-Yvon Fluorolog-3 spectrofluorimeter with Xe continuous (450 W) and pulsed (35W) lamps as excitation sources. The gas sensing chamber had been employed for testing of the films to gases. The dc electrical conductivity measurements were made on the experimental films by employing the standard van der Pauw method. The thermo emf of the prepared samples was studied between the temperature ranges from 275 to 325 K by using thermal probe method.

RESULTS AND DISCUSSION

SnO_2 thin films were prepared by using pulsed laser deposition method. The prepared thin films were characterized by SEM, TEM and PL studies to collect the information about the luminescent properties of the prepared sample. Gas sensing, electrical and thermal properties were also studied on to the prepared thin films. The analysis of X-ray diffraction pattern revealed that the prepared tin oxides films are pure crystalline in nature.

Morphological Studies

The morphology and chemical composition of as synthesized thin film was investigated by SEM and EDS analysis. Figure 1 shows the SEM micrographs of SnO_2 thin films taken with different magnifications. It can be clearly observed from low resolution SEM images that, the prepared sample show many agglomerates with an irregular morphology. The agglomeration could be induced by densification resulting from the narrow space between particles. SEM images reveal that the sample consists of irregular shaped sphere like structures. The observed EDS pattern was shown in Figure 2. The pattern showed the elemental compositions of Sn and O. TEM measurements were performed to confirm the nanocrystalline nature of the samples and to study the morphology of the particles. The TEM images of SnO_2 thin films are depicted in Figure 3. The particles are more or less uniformed in size and of irregular shape.

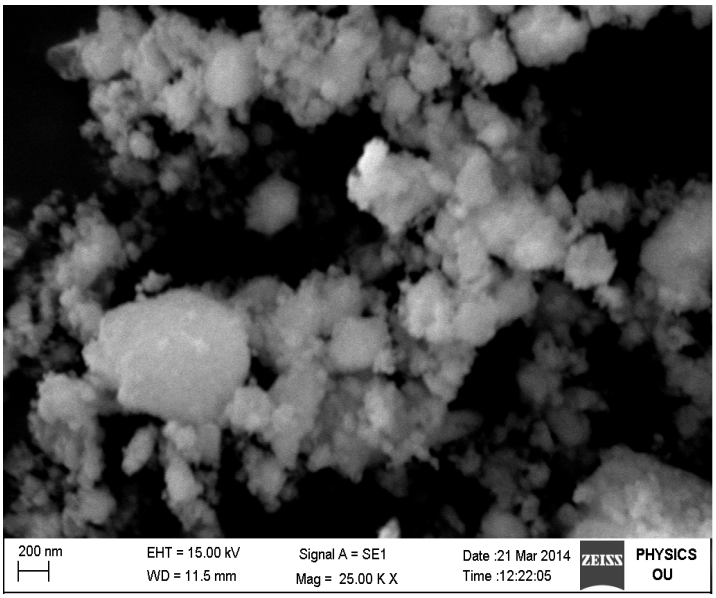

Figure 1: SEM image of SnO_2 thin films

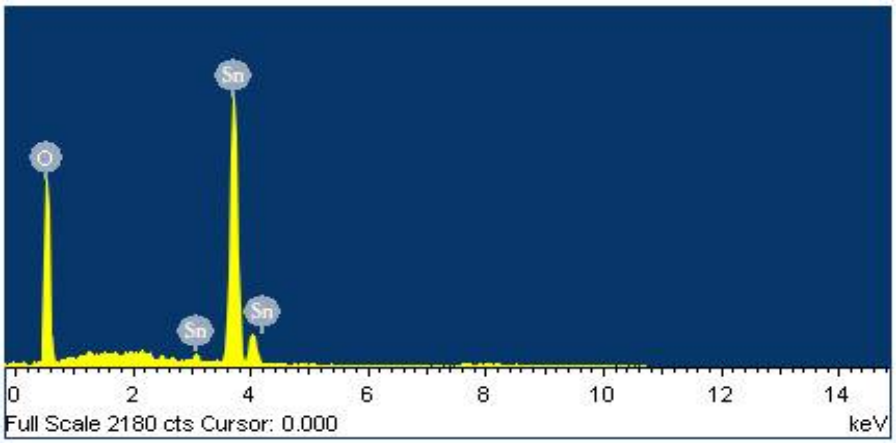

Figure 2: EDS spectrum of SnO_2 thin films

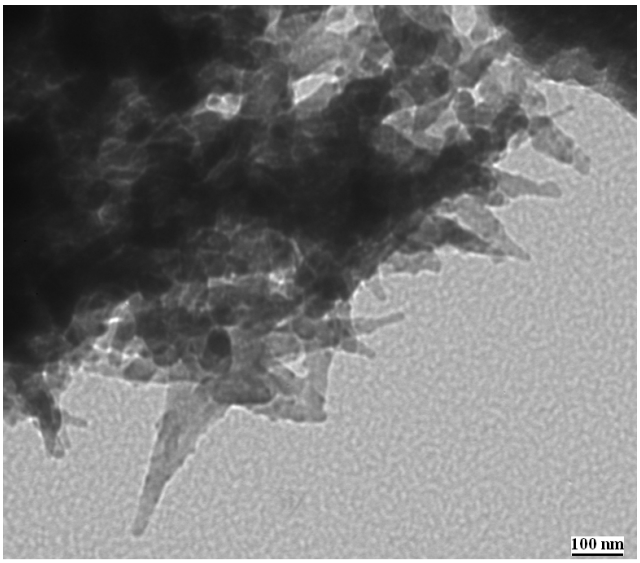

Figure 3: TEM image of SnO_2 thin films

Photoluminescence Studies

Photoluminescence (PL) phenomenon is directly related to electronic structure and transitions. Differences in the electronic behavior between bulk and low-dimensional semiconductors arise due to difference in the electronic density of states. PL emission spectrum of SnO_2 thin films under the photon excitation of 325 nm is shown in Figure 4.

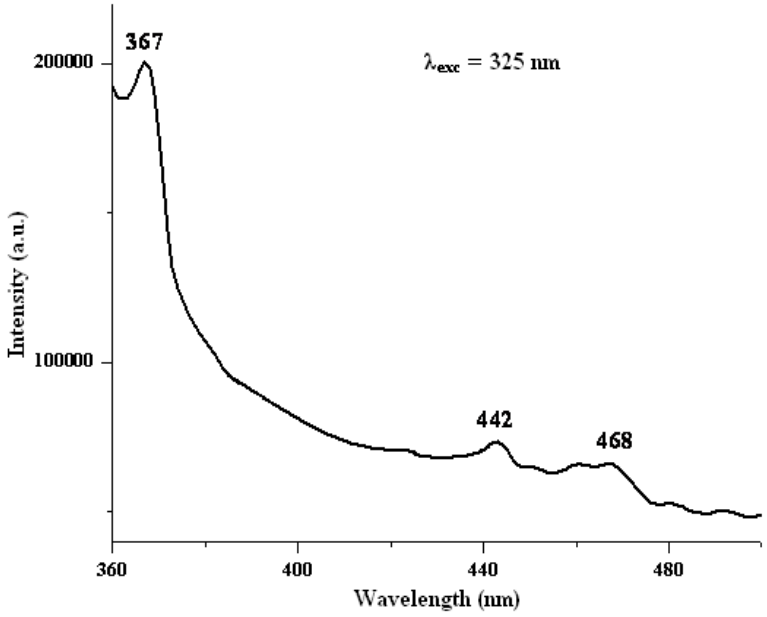

Figure 4: PL spectrum of SnO_2 thin films

PL emission having bands at 367, 442 and 468 nm are observed. An intense blue emission at 367 nm is a deep level emission usually appears due to surface effects [23]. An intense blue emission peak at around 367 nm is due to transition from conduction band of host to the "t_2" state and the green emission band at around 468 nm is from the shallow donor to the "t_2" state [24]. The prepared samples with blue emission are promising for applications in light emitting nanodevices [25].

Figure 5 shows the corresponding diagram of CIE 1931 chromaticity diagram SnO_2 thin films, the two axes being x and y chromaticity coordinates [26]. Location of the color coordinates are represented in the CIE chromaticity diagram by solid circle sign (•), which indicate the color of prepared sample. In the present investigation, calculated value of chromaticity index can be written as (x = 0.147, y = 0.124). From this figure, one can saw that the color of SnO_2 thin films were located in blue region. This material may be used in display devices [27, 28].

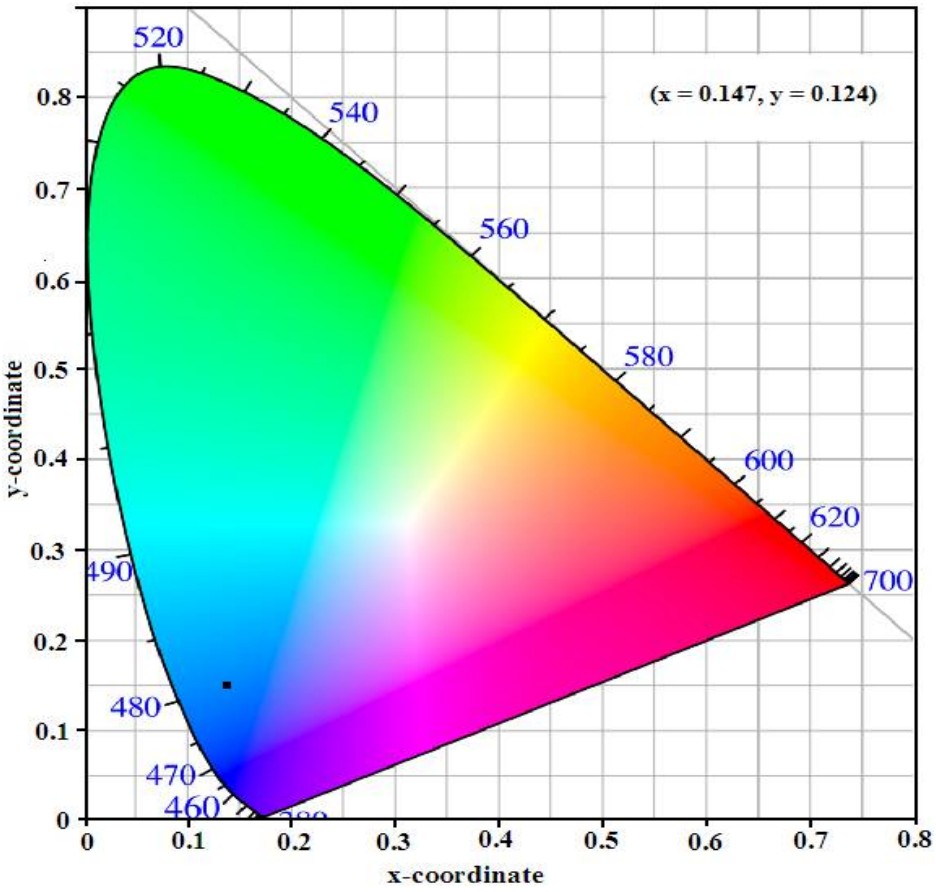

Figure 5: CIE diagram of SnO_2 thin films

Gas Sensing Properties

The conductance of the sensor in dry air was measured by means of conventional circuitary by applying constant voltage and measuring the current by picoammeter. The conductance was measured both in the presence and absence of test gas. The gas response (s) is defined as the ratio of change in conductance in gas to air to the original conductance in air

$S = (G_g – G_a) / G_a$

SnO_2 films were exposed to different concentrations of NO_2 gas at various temperatures. The sensor was placed in a stainless steel test chamber. A continuous flow of gas passes through the chamber, which makes the pressure in the test chamber to be nearly atmospheric. The desired gas concentration is obtained by mixing the appropriate flows of gases by means of mass flow controllers. The films are generally heat treated before exposure to different gasses because it produces contacts between grains, many of which are between grains having different crystal structures. When both the films are exposed to NO_2 gas, the dc electrical resistance of the film dramatically increased. Since SnO_2 is an n type semiconductor, its electrical behavior upon exposure of NO_2 oxidizing gas can be explained by a decrease of conduction carrier density. The amount of oxygen ions available on the SnO_2 surface increases at the operating temperature. The adsorbing NO_2 molecules interact directly with the adsorption sites at the oxide surface. Therefore the interaction between the film and NO_2 is as follows;

$NO_2+e^- \rightarrow NO^{2-}(ad)$

The interaction with NO_2 results in a decrease in the free electron concentration. The decrease in free carrier concentration causes a rise in the film resistance.

The sensitivity of the prepared SnO_2 thin films for various gas concentrations can be calculated from the equation defined as follows:

$S = R_a/R_g$

where S is the sensitivity, R_a is the resistance of a sensor in air medium and R_g is the resistance of a sensor in a test gas medium. The calculations were made by taking the resistance values at the time after which there was no significant decrease in the resistance. The results of the sensing experiments were graphically presented in Figure 6. When the reducing gas is exposed to the sensing element, it reduces the resistance of the material, which confirms the typical characteristic of a n-type material. It is clearly observed that, as the test gas concentration was increased the resistance decreased drastically.

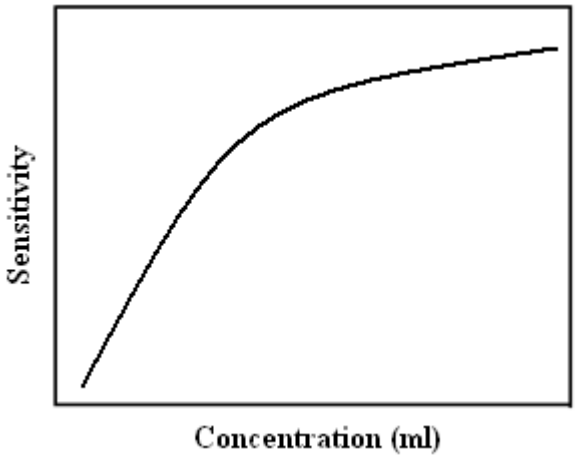

Figure 6: NO_2 concentration as a function of sensitivity of SnO_2 thin films

Electrical Properties

The electrical resistance of SnO_2 thin films was measured by the four - point probe method. The plot of log R as a function of reciprocal absolute temperature (1000/T) is found to consist of two linear parts shown in Figure 7.

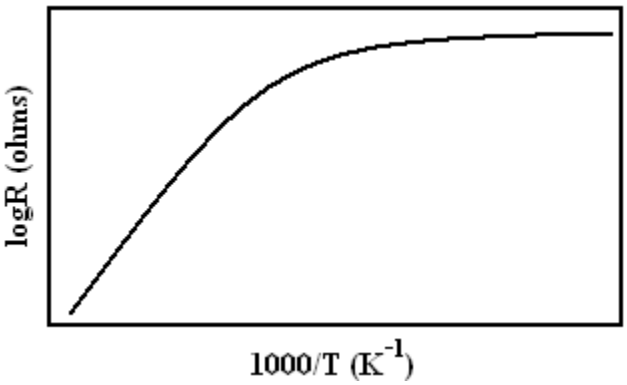

Figure 7: Plot of Log R versus 1000/T of SnO_2 thin films

The dc dielectric resistance is found to vary as

$R = R_0 \exp (\Delta E / KT)$

The presence of distinct values of ΔE in different temperature ranges may be attributed to two activation processes namely (1) it is intrinsic conduction at band gap in high temperature region and (2) in low temperature region, conduction is due to hopping of charge carriers in the localized states at Fermi level. The electrons may be promoted into these defects by giving electrical or optical energy thereby increasing the conductivity of the films [29-32].

Thermo emf

The temperature difference ΔT between the two ends of a material is small and then the thermo power of a material is defined approximately as:

$S = - \Delta V/\Delta T$

and a thermoelectric voltage of ΔV is seen at the terminals.

The thermo emf of SnO_2 thin films was studied in the temperature range from 275 K - 325 K by using thermal probe method. The thermo emf was measured and the Seebeck coefficient of the material was also calculated. The plot of thermo emf versus temperature difference between the two junctions is found to be linear (Figure 8) indicating that the temperature dependence of thermo emf is the characteristic conduction of SnO_2 thin films.

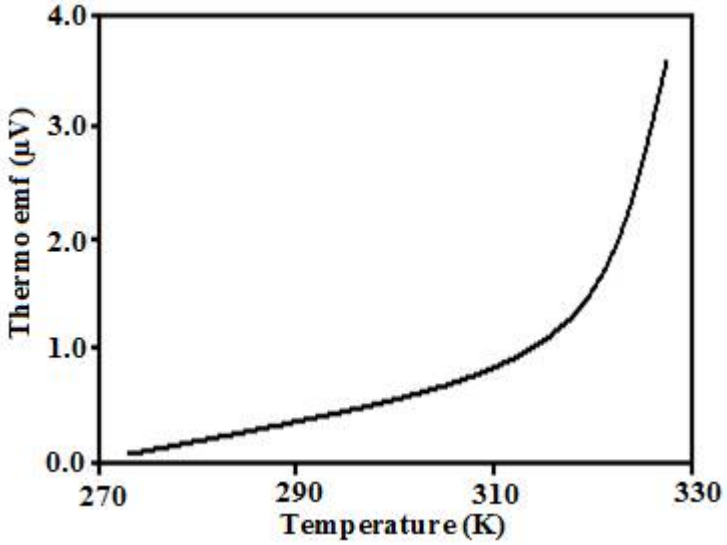

Figure 8: Temperature dependence of the thermo emf of SnO_2 thin films

The thermo emf of SnO_2 thin films increased with the increasing of temperature. At low temperatures the Seebeck coefficient is observed to be high and the Seebeck coefficient decreases with increasing of temperature. The large values of thermoelectric power of SnO_2 thin films are typical of semiconductor behavior.

CONCLUSION

SnO_2 thin films were prepared successfully by pulsed laser deposition method. SEM, EDS, TEM, PL, Gas sensing and Electrical properties were carried out on to the prepared thin films. SEM images taken at different magnifications clearly showed prepared sample contains irregular shaped nanoclusters with agglomeration. TEM images clearly show the formation of nano rods. PL spectrum of SnO_2 thin films shows blue emission. The calculated CIE coordinates of SnO_2 thin films were in blue region. Hence, SnO_2 thin films were expected to be useful in applications such as optoelectronics and lightening devices. SnO_2 films were exposed to different concentrations of NO_2 gas at various temperatures. The thermo emf of SnO_2 thin films increased with the increasing of temperature.

REFERENCES

[1] D.P. Norton, *Mater. Sci. Eng. R-Reports,* **2004,** 3, 139-145.
[2] M. Paranthaman, C. Park, X. Cui, A. Goyal, D.F. Lee, P.M. Martin, T.G. Chirayil, D.T. Verebelyi, D.P. Norton, D.K. Christen, D.M. Kroeger, *J. Mater. Res.*, **2000,** 15, 2647-2653.
[3] H.M. Christen, L.A. Boatner, J.D. Budai, M.F. Chisholm, L.A. Gea, P.J. Marrero, D.P. Norton, *Appl. Phys. Lett.*, **1996,** 68, 1488-1494.
[4] C.Y. Yang, S.E. Babcock, A. Goyal, M. Paranthaman, F.A. List, D.P. Norton, D.M. Kroeger, A. Ichinose, *Physica C,* **1998,** 307, 87-92.
[5] Y.E. Lee, D.P. Norton, J.D. Budai, *Appl. Phys. Lett*., **1999,** 74, 3155-3163.
[6] K. Ip, Y.W. Heo, D.P. Norton, S.J. Pearton, J.R. LaRoche, F. Ren, *Appl. Phys. Lett*., **2004,** 85, 1169-1176.
[7] S.K. Song, *Phys. Rev. B,* **1999,** 60, 11137-11143.
[8] M. Okuya, S. Kaneko, K. Hiroshima, I. Yagi, K. Murakami, *J. Eur. Ceram. Soc.*, **2001,** 21, 2099-2105.
[9] A. Khanna, R. Kumar, S.S. Bhatti, *Appl. Phys. Lett*., **2003,** 82, 4388-4396.
[10] M. Ivill, S.J. Pearton, D.P. Norton, J. Kelly, A.F. Hebard, *J. Appl. Phys*., **2005,** 97, 053904-053908.
[11] K. Ip, R.M. Frazier, Y.W. Heo, D.P. Norton, C.R. Abernathy, S.J. Pearton, J. Kelly, R. Rairigh, A.F. Hebard, J.M. Zavada, R.G. Wilson, *J. Vac. Sci. Technol. B*, **2003,** 21, 1476-1483.
[12] S.S. Park, J.D. Mackenzie, *Thin Solid Films*, **1995,** 258, 268-276.
[13] R.J. Choudhary, S.B. Ogale, S.R. Shinde, V.N. Kulkarni, T. Venkatesan, K.S. Harshavardhan, M.S.B. Hannoyer, *Appl. Phys. Lett*., **2004,** 84, 1483-1488.
[14] R.E. Cavicchi, S. Semancik, M.D. Antonik, R.J. Lad, *Appl. Phys. Lett*., **1992,** 61, 1921-1928.
[15] Y.R. Park, K.J. Kim, *J. Appl. Phys*., **2003,** 94, 6401-6407.
[16] J.C. Miller, R.F. Haglmel, Laser Ablation and Deposition, Academic Press, New York (1998).
[17] M.C. Rao, *J. Crys. Growth*, **2010**, 312, 2799–2803.
[18] M.C. Rao, *Optoelect. & Adv. Mater., (Rapid Commu.)*, **2011**, 5, 85-88.
[19] M.C. Rao**,** O.M. Hussain, *IOP Conf. Series: Mater. Sci. Eng.*, **2009**, 2, 012037 (p.1-4).
[20] M.C. Rao, *Optoelect. & Adv. Mater., (Rapid Commu.)*, **2011**, 5, 651-654.
[21] M.C. Rao, *J. Optoelect. & Adv. Mater*., **2011,** 13, 428-431.
[22] M.C. Rao, *Optoelect. & Adv. Mater.*, **2011,** 5, 85-92.
[23] S. Muthukumaran, R. Gopalakrishnan, *Opt. Mater.*, **2012,** 34, 1946-1952.
[24] B. Umesh, B. Eraiah, H. Nagabhushana, S.C. Sharma, B.M. Nagabhushana, C. Shivakumara, J.L. Rao, R.P.S. Chakradhar, *Spectrochim. Acta A,* **2012,** 94, 365-371.
[25] P. Yang, M. Lu, D. Xu, D. Yuan, G. Zhou, *Chem. Phys. Lett*., **2001,** 336, 76-82.
[26] P.R. Boyce, Human factors in lighting, 2nd Ed., Taylor and Francis Inc., New York (2003).
[27] S.M. Begum, K. Ravindranadh, M.C. Rao, RVSSN. Ravikumar, *J. Mol. Struct.*, **2011**, 1006, 344-347.
[28] S.M. Begum, M.C. Rao, RVSSN. Ravikumar, *J. Inorg. Organometa. Pol. Mat.* 2013, 23, 350-356.
[29] A.R. Patel, D.V. Mysorewala, *Mater. Res. Bull*., **1970,** 5, 1031-1038.
[30] C.A. Neugebauer, M.B. Webb, *J. Appl. Phys.* **1962,** 33, 74-79.
[31] M.C. Rao, O.M. Hussain, Research J. Chem. Sci., **2011**, 1, 92-95.
[32] M.C. Rao, J. Non-Oxide Glasses, **2013**, 5, 1-8.